Scientific Research Publishing

Atmospheric and Climate Sciences, 2025, 15(2), 289-313
https://www.scirp.org/journal/acs
ISSN Online: 2160-0422
ISSN Print: 2160-0414

# An Agroecological Zoning Approach for Sustainable Agriculture in Burkina Faso, West Africa

**Moussa Waongo[1], Ousmane Aly Yabyouré Ouedraogo[2], Abdoul Azise Sodoré[3], Sanoussi Atta[1]**

[1]Training and Research Department, AGRHYMET Regional Centre, Niamey, Niger
[2]Applied Meteorology Department, National Meteorological Agency, Ouagadougou, Burkina Faso
[3]Geography Department, Joseph KI-ZERBO University, Ouagadougou, Burkina Faso
Email: moussa.waongo@cilss.int

**How to cite this paper:** Waongo, M., Ouedraogo, O.A.Y., Sodoré, A.A. and Atta, S. (2025) An Agroecological Zoning Approach for Sustainable Agriculture in Burkina Faso, West Africa. *Atmospheric and Climate Sciences*, **15**, 289-313.
https://doi.org/10.4236/acs.2025.152014

**Received:** January 5, 2025
**Accepted:** February 4, 2025
**Published:** February 7, 2025



## Abstract

Agriculture in West Africa faces multiple challenges, such as climate variability, soil degradation, and limited access to reliable agroecological information for agricultural planning. In this context, traditional zonation approaches have often relied solely on rainfall patterns, potentially overlooking critical biophysical factors that influence agricultural productivity. This study presents a comprehensive agroecological zoning approach for Burkina Faso as a case study in West Africa, using multiple biophysical variables and k-means clustering analysis. The methodology integrates climate data from ERA5 reanalysis and TAMSAT satellite precipitation estimates, soil characteristics from the Harmonized World Soil Database, and derived agroclimatic indices for Burkina Faso for the period 1991-2020. Twelve variables, including precipitation, temperature, consecutive dry and wet days, onset and length of growing season, aridity index, and soil water content, were analyzed at 0.25˚ × 0.25˚ spatial resolution. The k-means clustering analysis identified four distinct agroecological zones (AEZs) with unique biophysical characteristics in Burkina Faso. The northern zone (AEZ1) exhibits semi-arid conditions, with longer dry spells and higher temperatures, while the southwestern zone (AEZ4) shows more favorable agricultural conditions with higher rainfall and longer growing seasons. The transitional zones (AEZ2 and AEZ3) display intermediate characteristics reflecting gradual changes in agroclimatic conditions. Comparison with the well-known rainfall-based zonation using the V-measure framework yielded a score of 0.55, indicating that the new AEZs incorporate additional biophysical factors resulting in more nuanced spatial differentiation for Burkina Faso. The methodology demonstrates the value of integrating multiple data sources and analytical approaches to better understand agricultural potential and constraints. This zonation provides a scientific basis for agricultural planning and policy development in Burkina Faso, with potential applications in other regions in West Africa facing similar agricultural challenges.

## Keywords

Agroecological Zones, k-Means Clustering, Climate Variability, Agricultural Planning, Burkina Faso, West Africa

## 1. Introduction

Agriculture is a crucial sector for food security in West Africa [1]. However, it is facing multiple challenges, such as the pressure on land resources, climate change, soil degradation, and water scarcity [2]-[4]. Indeed, in West Africa, cropping patterns and crop yields are driven by environmental factors, including climate and soil conditions and agricultural practices. Studies have shown that the capacity of the soil to provide nutrients for the optimum growth of plants is not only related to the amount of fertilizer but also to soil type and regional climate [5] [6]. According to these studies, plant-soil interaction is influenced by soil texture, water-holding capacity, and hydraulic conductivity, which shape nutrient availability to plants, and overall plant growth and development. Along the same line, climate conditions directly influence plant responses with regards to its impact on soil properties, water availability and nutrient availability [7]. The study of [8] has revealed that climate and soil are the main limiting factors of agricultural production in Africa. It is well known how soil characteristics, temperature and precipitation distribution can affect crop productivity, mainly in West Africa, where the agriculture system is dominated by rainfed agriculture with low use of fertilizers [5] [9] [10].

The uncertainty associated with climate variability and the lack or low accuracy in soil information reduces the investment and adoption of agricultural technologies. Indeed, specific temperatures are required for crop's optimal growth and development while high-temperature stress can adversely affect crop production [11] [12]. Precipitation distribution determines water availability for cropping and is the main driver for the length of crop growing period in Sub-Saharan Africa [13] [14]-[16]. Soil characteristics, along with climate, influence crop water availability through soil texture, structure, depth and water-holding capacity [17] [18]. In that context, the evaluation of the biophysical limitations and constraints is essential for identifying areas known as Agroecological Zones (AEZs) suitable for various crops or agricultural practices based on the climate and environmental characteristics of the land. Therefore, there is a growing interest in developing an agroecological zoning approaches that delineate regions as uniformly as possible with respect to soil, climate, and length of crop growing, therefore suited for integrating different aspects of farming systems to achieve sustainable agriculture [19]-[21].

The Food and Agriculture Organization of the United Nations (FAO) has developed an agronomically sound AEZ methodology in collaboration with the International Institute for Applied Systems Analysis (IIASA) [21]. This AEZ methodology makes use of global databases of climatic parameters, topography, soil, and terrain to assess land productivity. The importance of this work for sustainable agriculture was recognized by the 1983 FAO Conference [21]. The majority of AEZ approaches relied on the concepts of rainfall distribution, length of Growing Period (LGP), soil moisture and thermal regimes, which have been applied in mapping AEZ at various scales, from sub-national to global level, aiming to identify crop-specific limitations of prevailing climate [21]-[24]. However, the AEZ methodology faced challenges primarily associated with the availability and quality of datasets used to perform AEZ. At the regional scale across West Africa, accessing and ensuring the accuracy of location-specific biophysical data including climate, agronomic, and soil parameters remains a significant challenge [23].

Advances in satellite imaging and climate modeling techniques have substantially enhanced data assimilation, resulting in increasingly accurate and comprehensive databases [25]-[28]. The availability of these data at regional scale has supported their extensive use in West Africa in the context of the decline in weather observation networks and inconsistent reporting across West Africa [29]. Reference [30] has demonstrated that the European Centre for Medium-Range Weather Forecasts' fifth generation (ERA5) reanalysis data significantly reduced precipitation and temperature biases and better captured the annual cycle in the region's climatic zones, particularly precipitation in the Savannah and Guinea Coast and temperature in the Sahel. In addition, from the study of [28], among seven satellite-based rainfall estimates, TAMSAT v3.1 appears to be a good alternative source of precipitation data to rain gauge data over Burkina Faso.

In this context of enhanced quality of climate data collection in West Africa, improved accessibility to global databases containing climatic parameters, soil characteristics, and topographical information enables the derivation of key agro-meteorological parameters crucial for assessing the AEZs. Using Burkina Faso as a case study, we implement an approach that integrates climate variables, agro-meteorological and soil parameters, and clustering techniques to conduct a comprehensive AEZ assessment. This approach aims to enhance understanding of AEZs and promote sustainable agricultural practices in the region.

This study consists of three main sections. The first section addresses the data used in the study area and the data preprocessing. The second section presents the methodology used to perform the AEZ assessment. The outcomes of the study are presented and discussed in the last section.

## 2. Study Area and Datasets

### 2.1. Study Area

Burkina Faso (BF) is a landlocked country in West Africa, covering an area of

274,220 km². It is situated between 9.33˚ and 15.08˚ North latitude, and between 5.50˚ West and 2.33˚ East longitude. The country is bordered by six nations: Mali to the north, Niger to the east, Benin to the southeast, Togo and Ghana to the south, and Côte d'Ivoire to the southwest. The landscape is predominantly flat, with a mean altitude of approximately 300 meters above sea level (**Figure 1(a)**).

Two distinct seasons driven by the West African Monsoon are observed: a wet season (May to October), with a duration varying from three months in the north to six months in the south, and a dry season (November to April) dominated by the Harmattan, a warm and dry trade wind from the Sahara. The rainfall distribution follows a pronounced southward gradient, with annual precipitation varying from approximately 1200 mm in the southern regions to around 300 mm in the northern areas. Meanwhile, daily mean temperatures during the wet season range between 21˚C and 34˚C across the country [31].

Agriculture forms the backbone of Burkina Faso's economy, with agricultural areas unevenly distributed over the country, with a dominant area in southwestern Burkina Faso (**Figure 1(b)**). In 2013, cultivated areas represented approximately 39% of the country's total land area and 70% - 80% of the population engaged in agricultural activities, primarily in rural areas [32] [33]. The sector contributes more than 30% to the national GDP and serves as the primary source of income for the rural population [34]. The agricultural system is predominantly rainfed and subsistence-oriented, focusing on three main staple crops: sorghum (*Sorghum bicolor*), millet (Panicum sp.), and maize (*Zea mays* L.) [15]. Climate-related challenges significantly impact agricultural productivity, including irregular rainfall distribution, changes in planting dates, occurrences of long dry spells, and limited water availability for crop growth, collectively making food security one of the primary challenges facing the country.

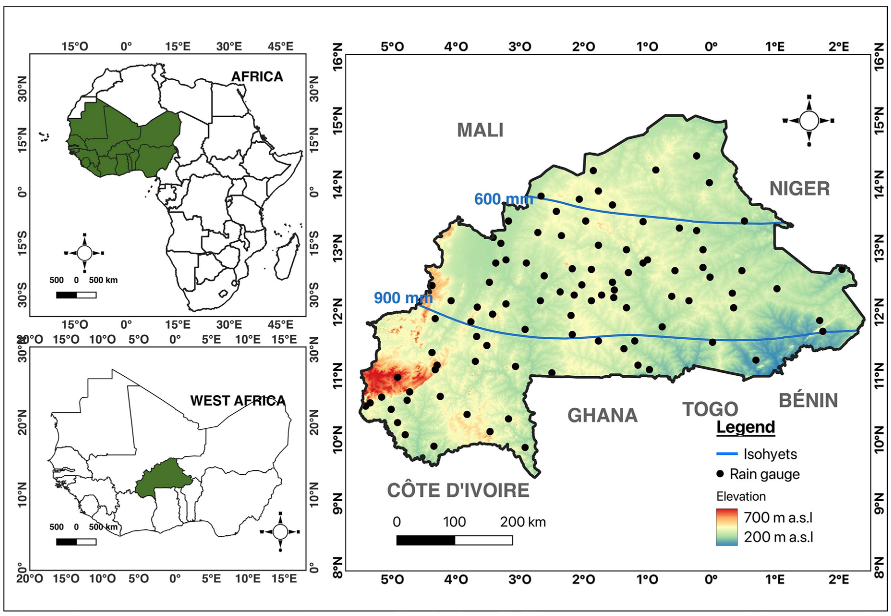


(a)

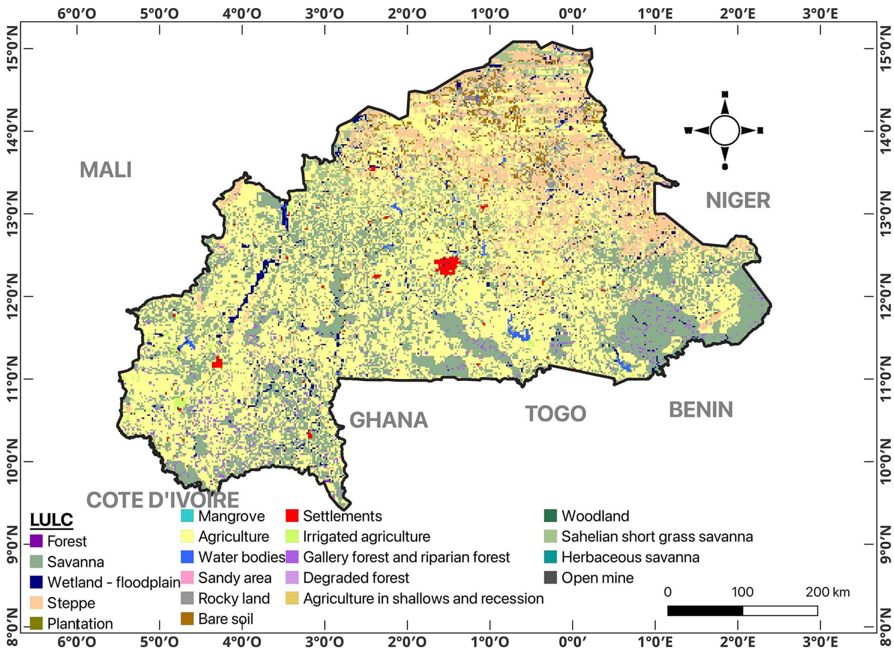


(b)

**Figure 1.** Geographical location of Burkina Faso along with spatial distribution of weather stations with annual precipitation distribution (a) and spatial distribution of dominant land use/land cover types across the country (b).

## 2.2. Climate Datasets

The proposed AEZ approach requires climate variables and agrometeorological parameters. Daily climate data at 0.25˚ × 0.25˚ spatial resolution for the period 1991-2020 were obtained from ERA5 reanalysis data [35]. The data include precipitation, minimum and maximum temperature, 2-meter dew point temperature, and surface net solar radiation. ERA5 has been widely validated and successfully applied in agricultural climate impact studies [36]-[38]. Additionally, satellite-derived precipitation datasets from TAMSAT v3.1 [28] for the period 1991-2020 were used. These satellite-based precipitation products have been extensively validated and applied for rainfall monitoring, crop assessment, and yield forecasting across various regions [28] [39] [40].

## 2.3. Soil Information

The soil texture is a fundamental physical property that significantly influences agricultural productivity and management practices. It refers to the relative proportions of sand, silt, and clay particles in soil, which directly affect crucial agricultural factors such as water retention and drainage, nutrient holding capacity and root development. In this study, soil parameters including organic carbon and the fractions of clay, silt, and sand were obtained from the latest version (2.0) of the Harmonized World Soil Database (HWSD) [41]. The dataset consists of raster files with a spatial resolution of 30 arc-seconds for six layers. The first five layers are 20 cm deep each, while the sixth layer is 50 cm deep. These data are further used to compute the dominant soil texture for each grid cell at 0.25˚ × 0.25˚ spatial resolution in the study area, based on the USDA soil classification [42]. It corresponds to the statistical mode of the sample of 2500 soil textures within the grid cell. Two soil variables have been considered in this study: topsoil (0 - 40 cm depth) and subsoil (40 - 100 cm depth).

# 3. Methodology

## 3.1. Reference Evapotranspiration Estimation

Reference evapotranspiration (ET0) plays a crucial role in agricultural and is essential for determining crop water requirements through the calculation of actual crop evapotranspiration (ETc) using crop coefficients [43]. ET0 also serves as a key input in agricultural drought monitoring and assessment. In this study, ET0 was computed using the FAO-Penman-Monteith method [44] with key meteorological variables retrieved from ERA5 reanalysis data at 0.25˚ × 0.25˚ resolution. The calculation integrates minimum and maximum near-surface air temperature, relative humidity, surface wind speed, and downwelling shortwave radiation, along with grid cell coordinates and Digital Elevation Model data (SRTM) as indicated in Equation (1).

$$\mathrm{ET0} = \frac{0.408 \times \Delta \times \left(R_n - G\right) + \gamma \times \dfrac{900}{T + 273} \times u_2 \times \left(e_s - e_a\right)}{\Delta + \gamma \times \left(1 + 0.32 \times u_2\right)} \quad (1)$$

where $R_n$ is the net radiation flux density on the crop surface (MJ·m$^{-2}$·d$^{-1}$); $G$ is the soil heat flux density (MJ·m$^{-2}$·d$^{-1}$); $T$ is the average daily air temperature (˚C); $u_2$ is the wind speed at 2 m high (m·s$^{-1}$); $e_s$ is the saturation vapor pressure (kPa); $e_a$ is the actual vapor pressure (kPa); Δ is the slope of vapor pressure-temperature curve (kPa·˚C$^{-1}$) and $\gamma$ is the psychometric constant (kPa·˚C$^{-1}$).

## 3.2. Agroclimatic Parameters Estimations

During the wet season, water availability for agriculture in West Africa, particularly in the Sahel region, is strongly influenced by the onset (ORS) and length (LOS) of the rainy season, as well as the intra-seasonal distribution of rainfall [45]. These factors are critical determinants of crop growth and productivity, especially in the Sahel dominated by rainfed agriculture. Prolonged dry spells can lead to drought conditions with adverse effects on agriculture, while frequent wet days affect plant water uptake and nutrient absorption. To characterize this intra-seasonal variability in precipitation, key metrics such as the length of dry spells (CDD), the frequency of wet days (CWD) and the number of wet days (NWD) are commonly utilized [46] [47].

In this study, five climate-related variables have been selected for the AEZ assessment: ORS, LOS, CWD, CDD and NWD. These variables were computed using wet-season precipitation data from TAMSAT_v3.1, following the definitions presented in **Table 1**. ORS and LOS were calculated using data from May to October, while CWD, CDD and NWD were computed on a monthly scale for the same period. For agricultural purposes and to minimize noise and errors associated with very light precipitation, a wet day was defined as a day with precipitation greater than or equal to 1 mm. This threshold helps address the challenge that satellite estimates often face in accurately detecting very light rainfall [48].

**Table 1.** Definitions of selected agroclimatic variable.

| Variables | Definitions | References |
|---|---|---|
| Onset of the rainy season (ORS) | The first date (expressed as day of the year) after May 1st when the following conditions are met:<br>1) At least 25 mm of rainfall accumulates over 5-day spell with at least two wet days (where a wet day has rainfall greater than or equal 1 mm).<br>2) No dry spell longer than 10 days occurs within the subsequent 30-day period | [15] |
| Length of the growing season (LOS) | $\mathrm{LS} = \sum_{i=1}^{n}\left(P_i - 0.5 \times \mathrm{ET0}_i\right) \geq 0$,<br>where $P_i$ represents precipitation for month $i$ and $\mathrm{ET0}_i$ denotes reference evapotranspiration for month $i$ | [49] |
| Number of wet days (NWD) | Number of days during which the daily precipitation amount is greater than or equal 1 mm | [14] |
| Dry spells length (CDD) | Maximum number of consecutive days with daily precipitation less than 1 mm | [50] |
| Wet spell length (CWD) | Maximum number of consecutive days with daily precipitation greater than or equal 1 mm | [50] |

## 3.3. Aridity Index

One widely accepted method of quantifying aridity is through the ratio of precipitation to potential evapotranspiration as shown in Equation (2) and known as the aridity index (AI). It provides valuable insights into the water balance of a region, reflecting the relationship between water availability through precipitation and atmospheric water demand through evapotranspiration [51]. In this study, AI has been computed at 0.25˚ × 0.25˚ resolution using ET0 computed from ERA5 reanalysis data and precipitation data from TAMSAT V3.1.

$$\mathrm{AI} = \frac{P_i}{\mathrm{ET0}_i} \tag{2}$$

where $P_i$ is the total precipitation for month $i$ and $\mathrm{ET0}_i$ is the monthly reference evapotranspiration.

## 3.4. Soil Water Content

Soil information from the Harmonized World Soil Database (HWSD) was used to determine the dominant soil texture at each grid cell according to USDA soil classification [42]. Using this dominant soil texture, we calculated the available soil water content (AWC) based on soil hydraulic characteristics for both topsoil and subsoil layers. The hydraulic parameters were obtained from the FAO soil hydraulic property database implemented in AquaCrop [52], which provides pre-calculated values for field capacity (FC) and permanent wilting point (PWP) corresponding to USDA textural classes. For each grid cell *i* and soil layer *j* associated with a specific soil texture, AWC was calculated using Equation (3).

$$\mathrm{AWC}_{ij} = \mathrm{FC}_{ij} - \mathrm{PWP}_{ij} \tag{3}$$

## 3.5. AEZ Based on k-Means Clustering

A k-means clustering method was applied to twelve variables, selected to prevent overweighting of redundant information in the study area. The k-means algorithm partitions datasets into a predefined number of clusters ($k$) based on similarity [53]-[55], minimizing within-cluster variance while maximizing between-cluster variance [56]. In this study, k-means clustering classified spatially distributed grid cells into distinct AEZs based on the variables presented in **Table 2**. The k-means clustering implementation for AEZ delineation involved three main steps. First, variables in **Table 2** were standardized using z-score normalization following Equation (4).

$$z_i = \frac{x_i - \mu}{\sigma} \tag{4}$$

where $z_i$ is the normalized value of the variable at grid cell $i$, $x_i$ is the value of the variable at grid cell $i$, and $\mu$ and $\sigma$ are the mean and standard deviation values of $x_i$ for the period 1991-2020, respectively.

Second, the optimal cluster number ($k$) was determined using the Elbow Method [57]. This method aims to identify the value of $k$ beyond which additional clusters do not substantially improve clustering performance, as measured by the within-cluster sum of squares (WCSS) as shown in Equation (5).

$$\mathrm{WCSS} = \sum_{j=1}^{k} \sum_{x_i \in C_j} \left\| x_i - \mu_j \right\|^2 \tag{5}$$

where $k$ is the number of clusters, $C_j$ represents the $j$-th cluster, $x_i$ is a grid cell belonging to cluster $C_j$, $\mu_j$ is the centroid of cluster $C_j$, $\left\| x_i - \mu_j \right\|$ is the Euclidean distance between $x_i$ and $\mu_j$. Lower WCSS values indicate better clustering performance, with WCSS = 0 representing perfect clustering.

Finally, the k-means algorithm assigned each grid cell to one of k clusters based on similarity in the selected variables. The algorithm minimized the total distance between grid cells and their respective cluster centroids, ensuring maximum within-cluster similarity. To address the sensitivity of k-means clustering to initial centroid locations and avoid local minima, the algorithm was iterated 25 times with different random initializations. The solution yielding the lowest WCSS was selected as the optimal clustering result [58]. Implementation, clustering analysis, visualization, and thematic map generation were performed using R, along with the R-packages "terra" and "tidyverse" [59]-[61].

## 3.6. Validation Against Rainfall Zones

Rainfall distribution is extensively used to delineate agroclimatic zones in West

Table 2. Selected climate, agroclimatic, and soil variables used in the study.

| Type | Name | Frequency | Source |
|---|---|---|---|
| climate | Precipitation (PCP) | Monthly | TAMSAT_v3.1 |
| | Minimum temperature (TN) | Monthly | ERA5 |
| | Maximum temperature (TX) | | |
| Agroclimatic | Onset of the rainy season (ORS) | Annual | TAMSAT_v3.1 |
| | Length of the growing season (LOS) | | |
| | Number of wet days (NWD) | Monthly | |
| | Dry spells length (CDD) | | |
| | Wet spell length (CWD) | | |
| | Aridity index (AI) | | |
| | Reference evapotranspiration (ET0) | Monthly | ERA5 |
| Soil | Topsoil water content (AWC_T) | Not Applicable | HWSD |
| | Subsoil water content (AWC_S) | | |

Africa. In Burkina Faso, the 600 mm and 900 mm isohyets (**Figure 1**) define three distinct agroclimatic zones: the Sahelian zone (rainfall < 600 mm), the Soudano-Sahelian zone (600 - 900 mm), and the Soudanian zone (>900 mm) [62]. To evaluate the correspondence between our derived AEZs and these established agroclimatic zones, we employed the V-measure, a composite metric combining Homogeneity and Completeness scores [63]. Homogeneity ($h$) quantifies whether each cluster contains members of a single class (Equation (6)).

$$h = 1 - \frac{H(C|K)}{H(C)}$$

$$H(C|K) = -\sum_{k\in K}\sum_{c\in C} P(c,k)\log\left(\frac{P(c,k)}{P(k)}\right) \tag{6}$$

$$H(C) = -\sum_{c\in C} P(c)\log P(c)$$

where $C$ represents the set of classes, $K$ represents the set of clusters, $P(c, k)$ denotes the probability that a grid cell belongs to both class $c$ and cluster $k$, $P(k)$ denotes the probability that a grid cell belongs to cluster $k$, and $P(c)$ denotes the probability that a grid cell belongs to class $c$.

Completeness ($c$) assesses whether all members of a given class are assigned to the same cluster (Equation (7))

$$c = 1 - \frac{H(K|C)}{H(K)}$$

$$H(K|C) = -\sum_{c\in C}\sum_{k\in K} P(c,k)\log\left(\frac{P(c,k)}{P(c)}\right) \tag{7}$$

$$H(K) = -\sum_{k\in K} P(k)\log P(k)$$

where $C$ represents the set of classes, $K$ represents the set of clusters, $P(c, k)$ denotes the probability that a grid cell belongs to both class $c$ and cluster $k$, $P(k)$

denotes the probability that a grid cell belongs to cluster $k$, and $P(c)$ denotes the probability that a grid cell belongs to class $c$.

The V-measure ($V$) is calculated as the harmonic mean of homogeneity and completeness (Equation (8))

$$V = \frac{(1+\beta)\times h\times c}{(\beta\times h)+c} \tag{8}$$

where $\beta$ is a weighting factor (typically $\beta = 1$ for equal weights). Both $h$ and $c$ range from 0.0 (worst) to 1.0 (perfect), with $V$ following the same scale.

## 4. Results

### 4.1. Intra-Seasonal Precipitation Variability

Figure 2 depicts the intra-seasonal variability of long-term mean precipitation across Burkina Faso from May to October for the period 1991-2020. A distinct spatiotemporal progression of precipitation is observed, characterized by a south-to-north gradient and marked monthly variations. May initiates the rainy season with lower precipitation levels (25 - 100 mm/month), while September marks the beginning of the seasonal decline, though significant precipitation (150 - 200 mm/month) persists across much of the country. The highest precipitation occurs during July and August, when rainfall reaches 200 - 300 mm/month in the south-west and south-central regions, while the northern areas receive 150 - 200 mm/month. By October, rainfall substantially decreases to 25 - 50 mm/month, with slightly higher amounts (50 - 100 mm/month) persisting only in the southwest.

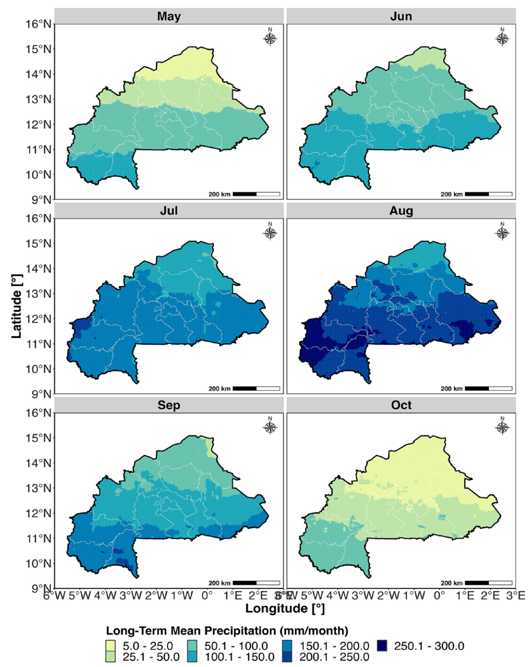


Figure 2. Spatial distribution of monthly precipitation across Burkina Faso during the rainy season (May-October), illustrating the seasonal migration of precipitation from south to north and maximum precipitation amounts during July-August.

### 4.2. Intra-Seasonal Temperature Variability

The spatial and temporal variation of long-term mean temperature across Burkina Faso from May to October, as presented in Figure 3, exhibits a persistent north-south temperature gradient throughout the growing season. A gradual temperature decrease occurs from June through August, with August showing the lowest temperatures (24˚C - 28˚C) nationwide. The highest temperatures occur in May, with temperatures ranging from 32˚C - 36˚C in the northern regions, while the south remains relatively cooler (28˚C - 30˚C). The southwestern region consistently maintains lower temperatures compared to the north.

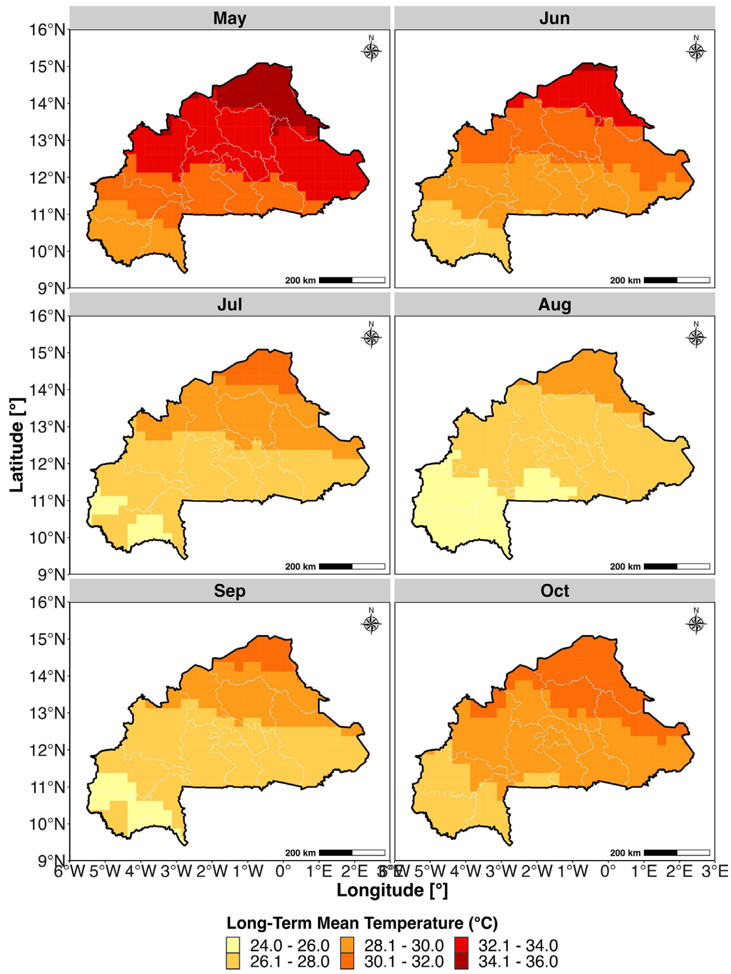


Figure 3. Spatiotemporal distribution of long-term mean monthly temperature over Burkina Faso during May-October, showing the north-south thermal gradient and its intra-seasonal evolution.

### 4.3. Reference Evapotranspiration

Figure 4 illustrates the spatial distribution of long-term mean ET0 across Burkina Faso, highlighting spatial variations and indicating monthly fluctuations of ET0 during May to October. The seasonal ET0 magnitude ranges from 5.0 to 6.0 mm/day, with maximum variability observed in the northern regions (4.0 to 10.0

mm/day) and minimum variability in the southwest (4.0 to 8.0 mm/day). May exhibits the highest ET0 values (9.1 to 10.0 mm/day), with the nationwide maximum reached in the northern regions. The north-south ET0 gradient is pronounced, particularly during May and October, while the southwestern region consistently maintains lower ET0 rates.

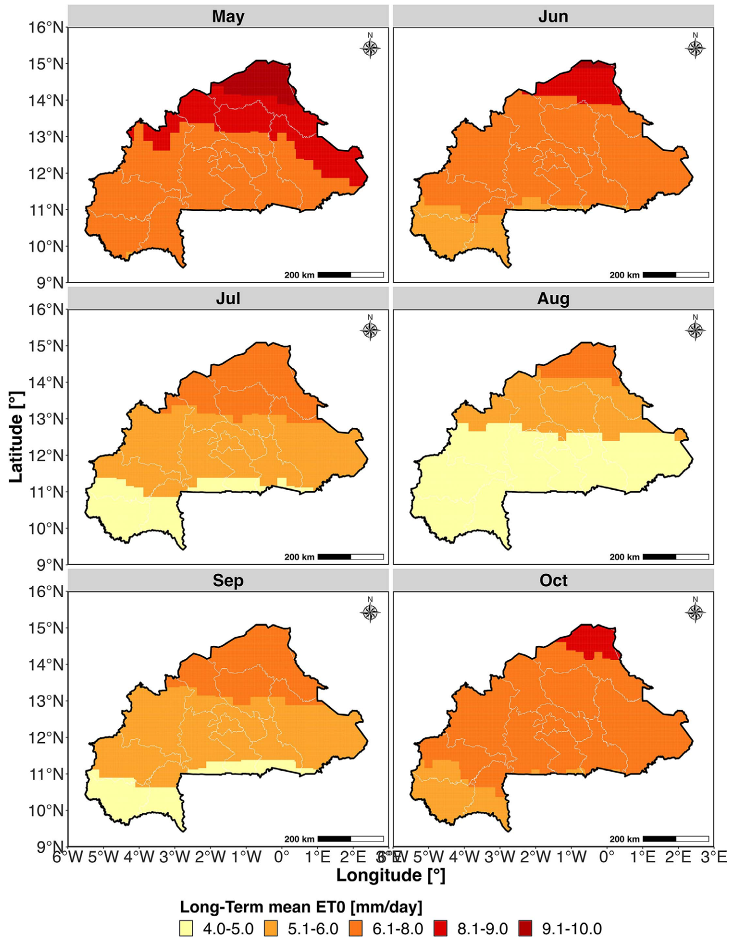


**Figure 4.** Monthly evolution of reference evapotranspiration (ET0) over Burkina Faso from May to October, showing pronounced spatial gradients and temporal variations.

## 4.4. Seasonal Agroclimatic Characteristics

**Figure 5** presents distinct spatial patterns in Burkina Faso's agroclimatic indicators calculated over the period 1991-2020. The onset of the rainy season (ORS) expressed as a day of year (DOY) extends northward from mid-May (DOY 141 - 160) in the southwest to late June (DOY 181 - 200) in the north, with greater variability (standard deviation greater than 20 days) in the northern regions compared to the south (standard deviation of 11 - 15 days). The length of growing season (LOS) displays a south-north gradient, ranging from 5 to 6 months in the southwestern region to 3 - 4 months in the northern regions. The aridity index (AI) shows a gradual transition from moderately humid (0.75 - 1.0) conditions in the southwest to drier conditions (0.25 - 0.50) in the north, with the highest variability (standard deviation of 0.41 - 0.60) along the western border. The standard deviation maps reveal increased temporal variability in the northern regions across all indicators.

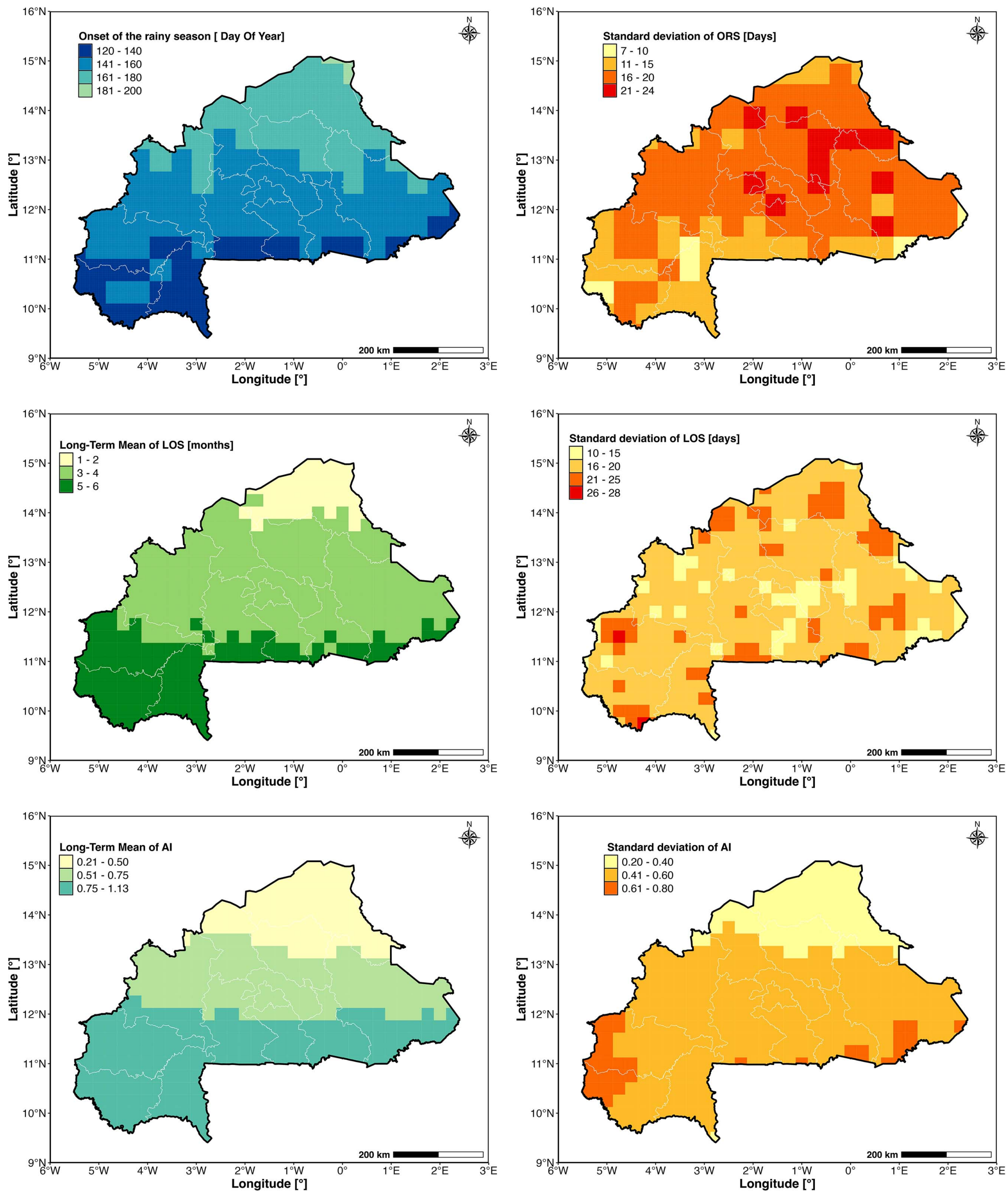


**Figure 5.** Long-term means (left) and standard deviations (right) of onset of the rainy season (ORS, top), length of growing season (LOS, middle), and aridity index (AI, bottom) in Burkina Faso over the period 1991-2020.

## 4.5. Wet and Dry Spell Variability

Spatial patterns of consecutive dry days (CDD), consecutive wet days (CWD), and number of wet days (NWD) show distinct climatic gradients across Burkina Faso during 1991-2020, as illustrated in Figure 6. CDD exhibits a north-south gradient, with longer dry spells (21 - 25 days) in the northern regions compared to shorter periods (5 - 10 days) in the south, with higher variability (standard deviation of 15 - 17 days) in the north. CWD displays an inverse pattern, with longer wet spells (6 - 7 days) in the southwestern region decreasing to 4 - 5 days in the northeast, while its temporal variability remains relatively uniform (standard deviation of 3 - 4 days) across the country. NWD demonstrates a pronounced southwest-north-east gradient, ranging from 80.1 - 90.0 days in the southwest to 35.1 - 50.0 days in the northeast, with moderate temporal variability (standard deviation of 11 - 15 days) throughout most of the country.

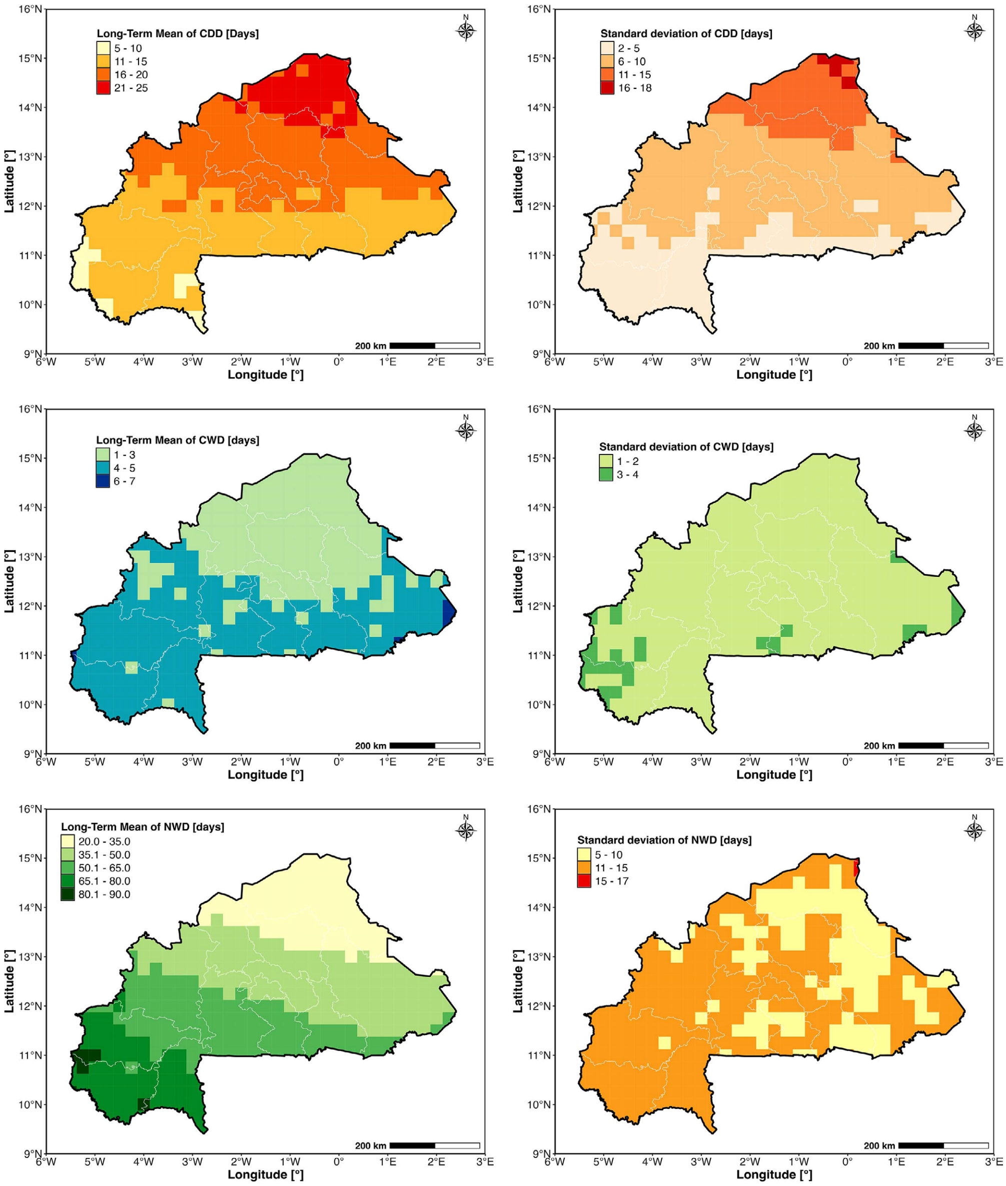


Figure 6. Long-term means (left) and standard deviations (right) of consecutive dry days (CDD, top), consecutive wet days (CWD, middle), and number of wet days (NWD, bottom) in Burkina Faso over the period 1991-2020.

### 4.6. Soil Texture and Water Content

Figure 7 shows the spatial distribution of soil texture and available water content (AWC) derived from soil textural properties across Burkina Faso. The topsoil (0 - 40 cm) is predominantly characterized by sandy loam and sandy clay loam textures, with scattered clay deposits in the central and eastern regions. The subsoil (40 - 100 cm) displays a similar textural pattern but with increased clay content, particularly in the southwestern and eastern areas. The calculated AWC shows a gradient from southwest to northeast, with topsoil values ranging from 20 to 50mm and higher capacity in the subsoil (30 - 85 mm). The subsoil exhibits notably higher AWC in the southwestern region (70 - 85 mm) compared to the northeastern areas (30 - 50 mm), corresponding to the variations in soil texture classes.

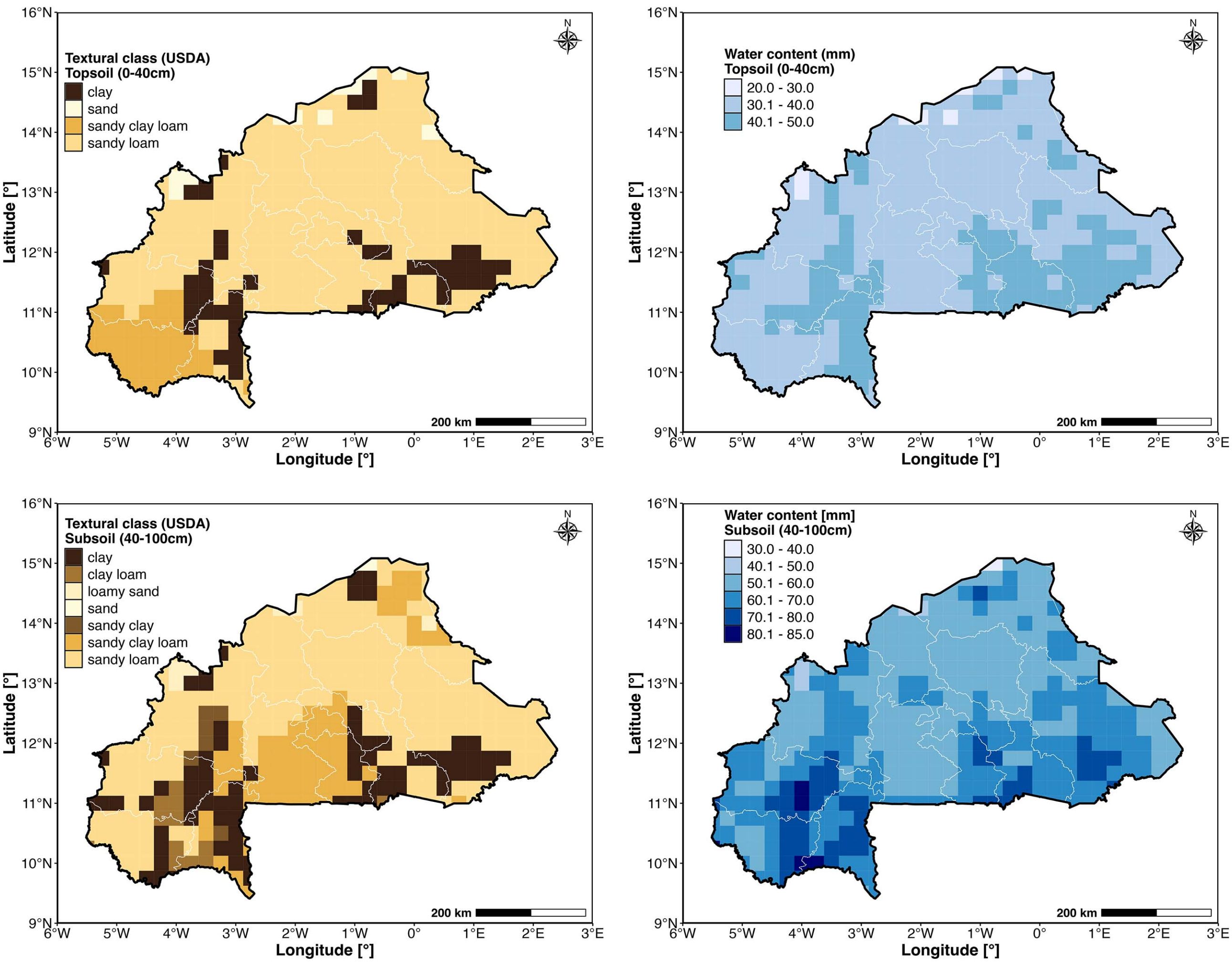


Figure 7. Soil textural classes (left) and derived available water content (right) for topsoil (0 - 40 cm, top) and subsoil (40 - 100 cm, bottom) in Burkina Faso.

### 4.7. Agroecological Zone Results

Figure 8 reveals the optimum *k* curve and the delineation of agroecological zones (AEZs) in Burkina Faso based on k-means clustering analysis of 12 biophysical variables. The elbow method indicates an optimal number of four clusters ($k = 4$), where the total within-cluster sum of squares shows a marked decrease until $k = 4$ (represented by the vertical dashed line) before leveling off. The resulting AEZs depict a clear latitudinal gradient, with AEZ4 covering the southwestern region, transitioning through AEZ3 and AEZ2 in the central areas, to AEZ1 in the northern zone.

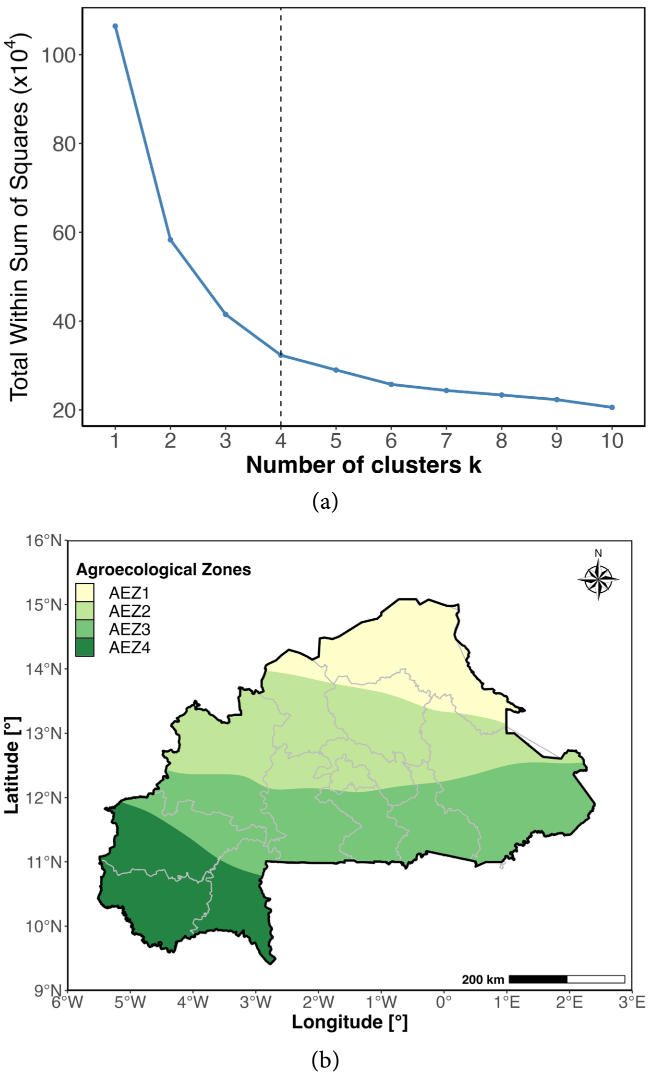


**Figure 8.** Optimal cluster analysis and spatial distribution of agroecological zones (AEZs) in Burkina Faso: elbow curve showing the optimal number of clusters (top) and spatial distribution of the four identified AEZs (bottom).

The characteristics of each AEZ through standardized indices of the 12 variables, calculated as deviations from the nationwide mean and normalized by the nationwide standard deviation are illustrated in Figure 9. For each AEZ, the values for each variable encompass the mean values of the variable for each gridcell belonging to the AEZ. The width of the boxplots within each zone indicates the spatial variability of these standardized indices across the gridcells within each

AEZ. From the boxplot analysis, AEZ1 shows longer dry spells (CDD), shorter growing seasons (LOS), and lower available soil water content in both topsoil and subsoil layers (AWC_T, AWC_S) than the national average, while consistently experiencing much lower rainfall (PCP), fewer wet days (NWD), coupled with higher maximum and minimum temperatures (TX, TN) than the country as a whole. The transitional zones (AEZ2 and AEZ3) display intermediate characteristics with distinct patterns: AEZ2 experiences slightly delayed onset of rains (ORS), longer dry spells (CDD), and shorter growing seasons (LOS) with somewhat lower precipitation and near-average AI values, while maintaining moderate temperatures around the national mean. AEZ3 exhibits growing seasons (LOS) slightly longer than the national mean, with near-average maximum and minimum temperatures. AEZ4 in the southwest is characterized by substantially higher rainfall (PCP), longer growing seasons (LOS), more frequent wet days (NWD), higher AI, and notably higher subsoil water content (AWC_S) than the national average, while experiencing shorter dry spells (CDD) and lower maximum and minimum temperatures (TX, TN) compared to countrywide conditions. All AEZs show lower internal variability of soil water content, particularly for the topsoil (AWC_T). The standardized aridity index (AI) shows higher spatial intra-AEZ variability with an average similar to the national average, except for AEZ4 which shows a mean value higher than the national mean.

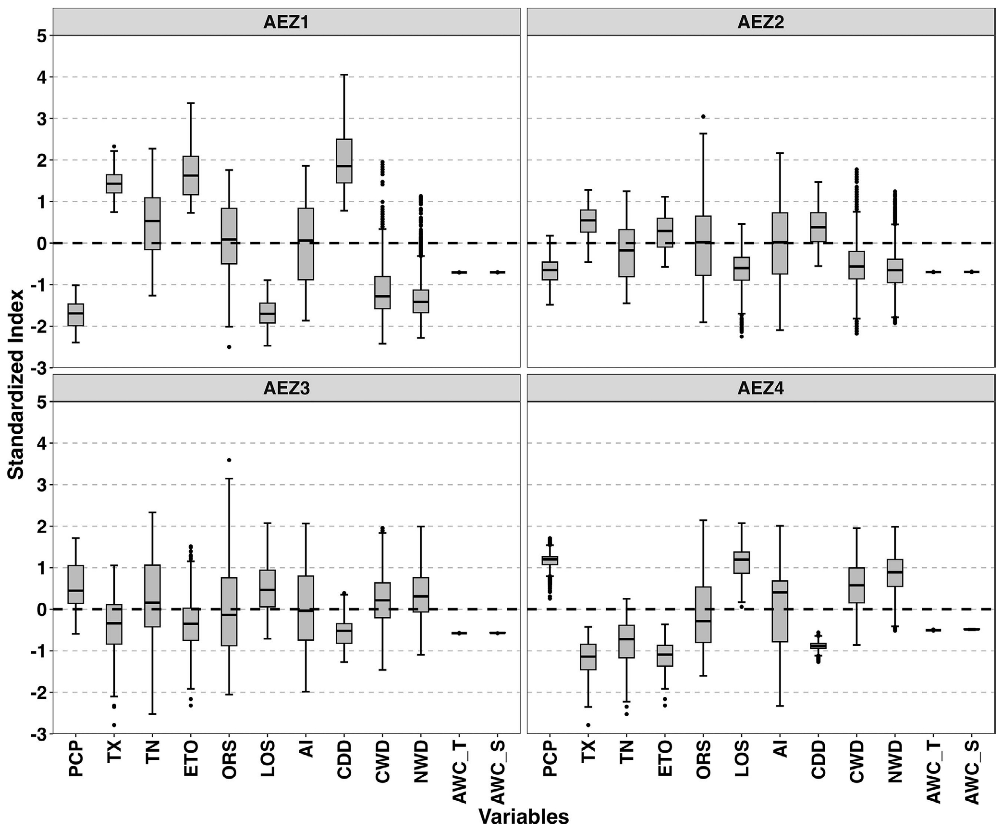


**Figure 9.** Variability of standardized indices for 12 biophysical variables within each of the agroecological zone of Burkina Faso.

### 4.8. AEZs against Rainfall-Based Zonation

The well-known rainfall-based zonation (Figure 10(a)) has been compared to our developed agroecological zones (AEZs) (Figure 10(b)) in Burkina Faso using the V-measure score. Both zonation approaches show distinct latitudinal bands, with the AEZs displaying a more refined southwestern region (AEZ4). The V-measure analysis shows a moderate agreement (V = 0.55) between the two zoning schemes, derived from a homogeneity score (h) of 0.62 and completeness score (c) of 0.50. This V-measure value indicates that the AEZ delineation captures a significant portion of the spatial patterns observed in the rainfall-based zones, but also introduces additional differentiation. The homogeneity maps (Figure 10(c), Figure 10(d)) reveal higher internal consistency (>0.7) in the northern regions for both classifications, while the central belt shows intermediate values (0.4 - 0.6). The relatively balanced V-measure components suggest that while the AEZs maintain the fundamental climatic gradients captured in the traditional zones, they incorporate additional biophysical factors that result in more nuanced spatial delineation, particularly in the differentiation of the southwestern region (AEZ4).

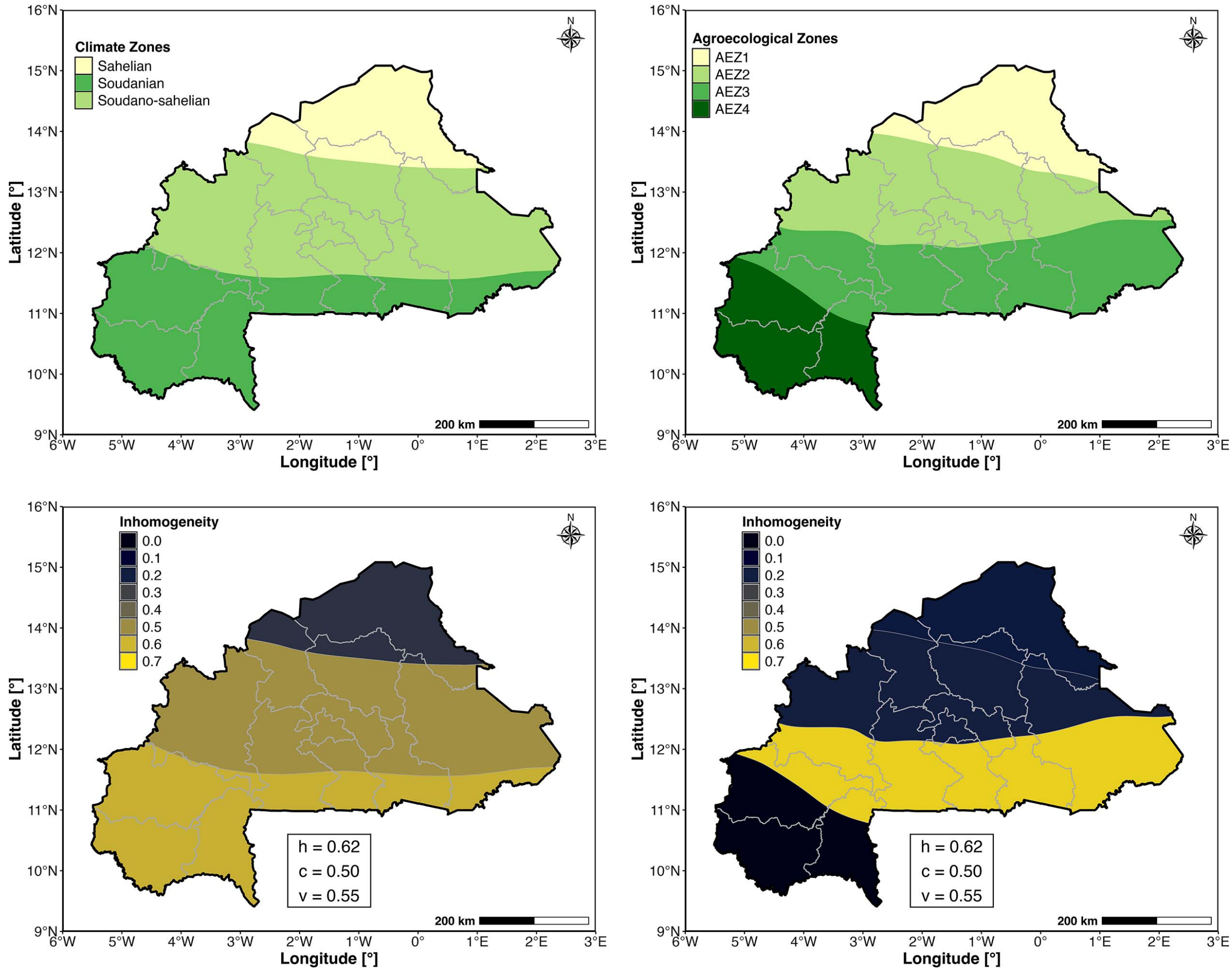


Figure 10. Comparison of rainfall-based zones (a) and agroecological zones (AEZs) (b) in Burkina Faso with their respective spatial homogeneity patterns and V-measure metrics (c, d).

## 5. Discussion

The analysis of agroecological zones (AEZs) in Burkina Faso reveals distinct spatial patterns shaped by the complex interactions between climatic, agroclimatic, and edaphic factors. The k-means clustering approach successfully identified four distinct AEZs (**Figure 8(b)**), each characterized by unique combinations of biophysical variables that demonstrate clear north-south gradients in most parameters (**Figure 9**).

The northern zone (AEZ1) exhibits characteristics typical of semi-arid regions [51], with significantly longer dry spells, shorter growing seasons, and higher temperatures compared to national averages. These conditions, combined with lower available soil water content, create substantial constraints for agricultural activities, particularly for rainfed agriculture which dominates the region [15]. The temporal variability in rainfall-related parameters is notably higher in this zone, indicating increased uncertainty in agricultural planning and potential risks for crop production [13] [14].

The transitional zones (AEZ2 and AEZ3) display intermediate characteristics but with distinct patterns that reflect their geographical position. AEZ2 shows characteristics that lean towards the northern zone's aridity, with delayed onset of rains and shorter growing seasons, while AEZ3 exhibits conditions more favorable for agriculture, with growing seasons slightly longer than the national average. These transitional zones play a crucial role in understanding the gradual shift in agricultural potential across the country [45] [46]. The moderate values across most variables in these zones suggest they might be particularly sensitive to climate variability and change, as small shifts in precipitation or temperature patterns could significantly impact agricultural outcomes [2] [3].

The southwestern zone (AEZ4) emerges as the most agriculturally favorable region, characterized by higher rainfall, longer growing seasons, and more frequent wet days. The lower temperatures and higher subsoil water content in this zone create conditions conducive to diverse agricultural practices [31] [32]. This aligns with the current distribution of agricultural areas in Burkina Faso, where the southwestern region hosts a significant portion of the country's farming activities [33] [34]. However, the higher spatial variability in the aridity index within this zone suggests potential localized challenges that require careful consideration in agricultural planning.

The soil characteristics across the AEZs add another layer of complexity to agricultural potential. The predominantly sandy loam and sandy clay loam textures influence water retention capabilities and nutrient availability [17] [18]. The variation in available water content between topsoil and subsoil layers, particularly pronounced in AEZ4, has important implications for crop root development and water accessibility throughout the growing season [5] [6]. The lower internal variability of soil water content across all AEZs, especially in the topsoil, suggests that soil characteristics provide a relatively stable foundation for agricultural planning, even as climatic variables show higher variability [7] [8].

The comparison between our AEZ delineation and well-known rainfall-based zonation yields important insights. The moderate V-measure score (0.55) indicates that while the AEZs capture fundamental climatic patterns, they also incorporate additional biophysical factors that result in more nuanced spatial differentiation. This is particularly evident in the southwestern region, where AEZ4 shows distinct characteristics that might be overlooked in simpler rainfall-based classifications [62]. The balanced homogeneity (0.62) and completeness (0.50) scores suggest that the AEZ approach successfully maintains the integrity of established climatic boundaries while providing additional resolution in agricultural potential assessment.

Our findings have several important implications for agricultural planning and development in Burkina Faso. First, the clear spatial differentiation in growing season characteristics (onset, length, and variability) suggests the need for zone-specific agricultural calendars and crop selection strategies [15] [16]. Second, the varying levels of climatic variability across zones, particularly in rainfall-related parameters, highlight the importance of developing risk management strategies tailored to local conditions [13] [14]. Third, the interaction between climatic and soil characteristics, especially evident in water availability patterns, emphasizes the need for integrated approaches to agricultural water management [5] [9].

These results also have broader implications for agricultural development in West Africa. The methodology demonstrated here, combining multiple data sources and clustering techniques, provides a framework for detailed agroecological zonation that could be applied in other regions facing similar agricultural challenges [21] [22]. The successful integration of satellite-derived data and reanalysis products [28] [30] offers a practical approach for regions where ground-based observations are limited [29].

However, several limitations should be considered. First, while the spatial resolution of our analysis ($0.25^\circ \times 0.25^\circ$) provides useful insights at the regional scale, it may mask local-level variations important for farm-level decision-making. Second, the static nature of soil property data might not fully capture temporal changes in soil characteristics. Our approach effectively captures spatial patterns of soil properties but fails to account for temporal changes driven by land use conversion, soil erosion processes, and increasing anthropogenic pressures in the context of climate change in the region.

Third, the k-means clustering algorithm, while widely used, is sensitive to initialization and may converge to local optima [58]. Although using 25 random initializations and selecting the solution with the lowest within-cluster sum of squares improves stability, the risk of getting local optima cannot be discarded. Fourth, the analysis focuses on current conditions and does not explicitly address future climate change scenarios, which could significantly alter the characteristics and boundaries of these AEZs [2] [4].

## 6. Conclusion

This study provides a comprehensive characterization of agroecological zones in

Burkina Faso based on multiple biophysical factors. The results demonstrate the value of integrating various data sources and analytical approaches to better understand agricultural potential and constraints. The identified zones and their characteristics offer a scientific basis for agricultural planning and policy development, while the methodology provides a framework for similar analyses in other regions. Future research could focus on incorporating climate change projections, higher resolution data sources, and additional biophysical parameters to further refine our understanding of agroecological zones and their implications for sustainable agriculture in West Africa.

## Acknowledgements

This work was funded by the German Federal Ministry of Education and Research (BMBF) research project CONCERT (grant number 01LG2101A) through the West African Science Center for Climate Change and Adapted Land Use (WASCAL). The authors gratefully acknowledge the European Centre for Medium-Range Weather Forecasts (ECMWF) for providing open access to ERA5 reanalysis data through the Copernicus Climate Change Service (C3S), and the University of Reading for making TAMSAT data freely available to the scientific community. We also acknowledge the anonymous reviewers for their availability and valuable comments.

## Conflicts of Interest

The authors declare no conflicts of interest regarding the publication of this paper.

## References

[1] Modi, R. (2018) The Role of Agriculture for Food Security and Poverty Reduction in Sub-Saharan Africa. In: Shaw, T.M., Mahrenbach, L.C., Modi, R., and Yi-Chong, X., Eds., *The Palgrave Handbook of Contemporary International Political Economy*, Palgrave Macmillan UK, 391-410. https://doi.org/10.1057/978-1-137-45443-0_25

[2] Douxchamps, S., Van Wijk, M.T., Silvestri, S., Moussa, A.S., Quiros, C., Ndour, N.Y.B., *et al.* (2015) Linking Agricultural Adaptation Strategies, Food Security and Vulnerability: Evidence from West Africa. *Regional Environmental Change*, **16**, 1305-1317. https://doi.org/10.1007/s10113-015-0838-6

[3] McIntire, J.M. (2014) Transforming African Agriculture. *Global Journal of Emerging Market Economies*, **6**, 145-179. https://doi.org/10.1177/0974910114525697

[4] Saghir, J. (2014) Global Challenges in Agriculture and the World Bank's Response in Africa. *Food and Energy Security*, **3**, 61-68. https://doi.org/10.1002/fes3.43

[5] Mbava, N., Mutema, M., Zengeni, R., Shimelis, H. and Chaplot, V. (2020) Factors Affecting Crop Water Use Efficiency: A Worldwide Meta-Analysis. *Agricultural Water Management*, **228**, Article ID: 105878. https://doi.org/10.1016/j.agwat.2019.105878

[6] Nisa, K.U., Tarfeen, N., Nisa, Q. and Wani, S. (2023) Climate Change and Plant Nutrient Availability: Challenges and Assessment Strategies. In: Aftab, T. and Hakeem, K.R., Eds., *Sustainable Plant Nutrition*, Elsevier, 71-86. https://doi.org/10.1016/b978-0-443-18675-2.00015-8

[7] Mengistu, T. (2020) Relationship between Climate Change and Crop Productivity: Review Articles. *International Journal of Research in Agronomy*, **3**, 55-61. https://doi.org/10.33545/2618060x.2020.v3.i1a.74

[8] Kurukulasuriya, P. and Mendelsohn, R.O. (2008) How Will Climate Change Shift Agro-Ecological Zones and Impact African Agriculture? Social Science Research Network, Report No. 4717, 31.

[9] Roudier, P., Sultan, B., Quirion, P. and Berg, A. (2011) The Impact of Future Climate Change on West African Crop Yields: What Does the Recent Literature Say? *Global Environmental Change*, **21**, 1073-1083. https://doi.org/10.1016/j.gloenvcha.2011.04.007

[10] Waha, K., Müller, C. and Rolinski, S. (2013) Separate and Combined Effects of Temperature and Precipitation Change on Maize Yields in Sub-Saharan Africa for Mid- to Late-21st Century. *Global and Planetary Change*, **106**, 1-12. https://doi.org/10.1016/j.gloplacha.2013.02.009

[11] Chen, Z., Galli, M. and Gallavotti, A. (2022) Mechanisms of Temperature-Regulated Growth and Thermotolerance in Crop Species. *Current Opinion in Plant Biology*, **65**, Article ID: 102134. https://doi.org/10.1016/j.pbi.2021.102134

[12] Hatfield, J.L. and Prueger, J.H. (2015) Temperature Extremes: Effect on Plant Growth and Development. *Weather and Climate Extremes*, **10**, 4-10. https://doi.org/10.1016/j.wace.2015.08.001

[13] Joseph, J.E., Akinseye, F.M., Worou, O.N., Faye, A., Konte, O., Whitbread, A.M., *et al.* (2023) Assessment of the Relations between Crop Yield Variability and the Onset and Intensity of the West African Monsoon. *Agricultural and Forest Meteorology*, **333**, Article ID: 109431. https://doi.org/10.1016/j.agrformet.2023.109431

[14] Laux, P., Kunstmann, H. and Bárdossy, A. (2008) Predicting the Regional Onset of the Rainy Season in West Africa. *International Journal of Climatology*, **28**, 329-342. https://doi.org/10.1002/joc.1542

[15] Waongo, M., Laux, P., Traoré, S.B., Sanon, M. and Kunstmann, H. (2014) A Crop Model and Fuzzy Rule Based Approach for Optimizing Maize Planting Dates in Burkina Faso, West Africa. *Journal of Applied Meteorology and Climatology*, **53**, 598-613. https://doi.org/10.1175/jamc-d-13-0116.1

[16] Ngetich, K.F., Mucheru-Muna, M., Mugwe, J.N., Shisanya, C.A., Diels, J. and Mugendi, D.N. (2014) Length of Growing Season, Rainfall Temporal Distribution, Onset and Cessation Dates in the Kenyan Highlands. *Agricultural and Forest Meteorology*, **188**, 24-32. https://doi.org/10.1016/j.agrformet.2013.12.011

[17] Gregory, P.J., Simmonds, L.P. and Pilbeam, C.J. (2000) Soil Type, Climatic Regime, and the Response of Water Use Efficiency to Crop Management. *Agronomy Journal*, **92**, 814-820. https://doi.org/10.2134/agronj2000.925814x

[18] Saxton, K.E., Rawls, W.J., Romberger, J.S. and Papendick, R.I. (1986) Estimating Generalized Soil-Water Characteristics from Texture. *Soil Science Society of America Journal*, **50**, 1031-1036. https://doi.org/10.2136/sssaj1986.03615995005000040039x

[19] Altieri, M.A. (2002) Agroecology: The Science of Natural Resource Management for Poor Farmers in Marginal Environments. *Agriculture, Ecosystems & Environment*, **93**, 1-24. https://doi.org/10.1016/s0167-8809(02)00085-3

[20] Gliessman, S. (2018) Defining Agroecology. *Agroecology and Sustainable Food Systems*, **42**, 599-600. https://doi.org/10.1080/21683565.2018.1432329

[21] Fischer, G., van Velthuizen, H.T. and Nachtergaele, F.O. (2000 Nov) Global Agro-Ecological Zones Assessment: Methodology and Results. IIASA, Report No. IR-00-064, 338.

[22] Pal, D.K., Mandal, D.K., Bhattacharyya, T., Mandal, C. and Sarkar, D. (2009) Revisiting the Agro-Ecological Zones for Crop Evaluation. *Indian Journal of Genetics and Plant Breeding*, **69**, 315-318.

[23] Seo, S.N. (2014) Evaluation of the Agro-Ecological Zone Methods for the Study of Climate Change with Micro Farming Decisions in Sub-Saharan Africa. *European Journal of Agronomy*, **52**, 157-165. https://doi.org/10.1016/j.eja.2013.09.014

[24] Ahmad, L., Habib Kanth, R., Parvaze, S. and Sheraz Mahdi, S. (2017) Agro-Climatic and Agro-Ecological Zones of India. In: Ahmad, L., Habib Kanth, R., Parvaze, S. and Sheraz Mahdi, S., Eds., *Experimental Agrometeorology*: *A Practical Manual*, Springer International Publishing, 99-118. https://doi.org/10.1007/978-3-319-69185-5_15

[25] Kidd, C., Levizzani, V. and Bauer, P. (2009) A Review of Satellite Meteorology and Climatology at the Start of the Twenty-First Century. *Progress in Physical Geography*: *Earth and Environment*, **33**, 474-489. https://doi.org/10.1177/0309133309346647

[26] Dee, D.P., Uppala, S.M., Simmons, A.J., Berrisford, P., Poli, P., Kobayashi, S., *et al*. (2011) The Era-Interim Reanalysis: Configuration and Performance of the Data Assimilation System. *Quarterly Journal of the Royal Meteorological Society*, **137**, 553-597. https://doi.org/10.1002/qj.828

[27] Reichstein, M., Camps-Valls, G., Stevens, B., Jung, M., Denzler, J., Carvalhais, N., *et al*. (2019) Deep Learning and Process Understanding for Data-Driven Earth System Science. *Nature*, **566**, 195-204. https://doi.org/10.1038/s41586-019-0912-1

[28] Maidment, R.I., Grimes, D., Black, E., Tarnavsky, E., Young, M., Greatrex, H., *et al*. (2017) A New, Long-Term Daily Satellite-Based Rainfall Dataset for Operational Monitoring in Africa. *Scientific Data*, **4**, Article No. 170063. https://doi.org/10.1038/sdata.2017.63

[29] Washington, R., Harrison, M., Conway, D., Black, E., Challinor, A., Grimes, D., *et al*. (2006) African Climate Change: Taking the Shorter Route. *Bulletin of the American Meteorological Society*, **87**, 1355-1366. https://doi.org/10.1175/bams-87-10-1355

[30] Gbode, I.E., Babalola, T.E., Diro, G.T. and Intsiful, J.D. (2023) Assessment of ERA5 and Era-Interim in Reproducing Mean and Extreme Climates over West Africa. *Advances in Atmospheric Sciences*, **40**, 570-586. https://doi.org/10.1007/s00376-022-2161-8

[31] Sivakumar, M.V.K. and Gnoumou, F. (1987) Agroclimatology of West Africa: Burkina Faso. International Crops Research Institute for the Semi-Arid Tropics.

[32] Zidouemba, P. (2017) Economy-Wide Implications of Climate Change in Burkina Faso. *Economics Bulletin*, **37**, 2797-808.

[33] Tappan, G.G., Cushing, W.M., Cotillon, S.E., Hutchinson, J.A., Pengra, B., Alfari, I. *et al*. (2016) Landscapes of West Africa: A Window on a Changing World. USGS, 82-89. https://doi.org/10.5066/F7N014QZ

[34] Diao, X., Hazell, P., Danielle, R. and James, T. (2007) The Role of Agriculture in Development: Implications for Sub-Saharan Africa. International Food Policy Research Institute.

[35] Bell, B., Hersbach, H., Simmons, A., Berrisford, P., Dahlgren, P., Horányi, A., *et al*. (2021) The ERA5 Global Reanalysis: Preliminary Extension to 1950. *Quarterly Journal of the Royal Meteorological Society*, **147**, 4186-4227. https://doi.org/10.1002/qj.4174

[36] Rolle, M., Tamea, S. and Claps, P. (2022) Climate-Driven Trends in Agricultural Water Requirement: An ERA5-Based Assessment at Daily Scale over 50 Years. *Environ-*

*mental Research Letters*, **17**, Article ID: 044017. https://doi.org/10.1088/1748-9326/ac57e4

[37] Rolle, M., Tamea, S. and Claps, P. (2021) ERA5-Based Global Assessment of Irrigation Requirement and Validation. *PLOS ONE*, **16**, e0250979. https://doi.org/10.1371/journal.pone.0250979

[38] Zhang, R., Li, L., Zhang, Y., Huang, F., Li, J., Liu, W., *et al.* (2021) Assessment of Agricultural Drought Using Soil Water Deficit Index Based on ERA5-Land Soil Moisture Data in Four Southern Provinces of China. *Agriculture*, **11**, Article 411. https://doi.org/10.3390/agriculture11050411

[39] Asfaw, D., Black, E., Brown, M., Nicklin, K.J., Otu-Larbi, F., Pinnington, E., *et al.* (2018) TAMSAT-ALERT V1: A New Framework for Agricultural Decision Support. *Geoscientific Model Development*, **11**, 2353-2371. https://doi.org/10.5194/gmd-11-2353-2018

[40] Dembélé, M. and Zwart, S.J. (2016) Evaluation and Comparison of Satellite-Based Rainfall Products in Burkina Faso, West Africa. *International Journal of Remote Sensing*, **37**, 3995-4014. https://doi.org/10.1080/01431161.2016.1207258

[41] FAO and IIASA (2023) Harmonized World Soil Database Version 2.0. FAO, International Institute for Applied Systems Analysis (IIASA). https://doi.org/10.4060/cc3823en

[42] Moreno-Maroto, J.M. and Alonso-Azcárate, J. (2022) Evaluation of the USDA Soil Texture Triangle through Atterberg Limits and an Alternative Classification System. *Applied Clay Science*, **229**, Article ID: 106689. https://doi.org/10.1016/j.clay.2022.106689

[43] Dalezios, N.R., Dercas, N., Faraslis, I.N., Spiliotopoulos, M., Sidiropoulos, P., Sakelariou, S., *et al.* (2023) Irrigation and Agrometeorology: Innovative Remote Sensing Applications in Crop Monitoring. In: Eslamian, S. and Eslamian, F., Eds., *Handbook of Irrigation Hydrology and Management*, CRC Press, 243-259. https://doi.org/10.1201/9780429290114-15

[44] Allen, R.G., Pereira, L.S., Raes, D. and Smith, M. (1998) Crop Evapotranspiration—Guidelines for Computing Crop Water Requirements—FAO Irrigation and Drainage Paper 56. Food and Agriculture Organization.

[45] Laux, P., Jäckel, G., Tingem, R.M. and Kunstmann, H. (2010) Impact of Climate Change on Agricultural Productivity under Rainfed Conditions in Cameroon—A Method to Improve Attainable Crop Yields by Planting Date Adaptations. *Agricultural and Forest Meteorology*, **150**, 1258-1271. https://doi.org/10.1016/j.agrformet.2010.05.008

[46] Ibrahim, B., Polcher, J., Karambiri, H. and Rockel, B. (2012) Characterization of the Rainy Season in Burkina Faso and It's Representation by Regional Climate Models. *Climate Dynamics*, **39**, 1287-1302. https://doi.org/10.1007/s00382-011-1276-x

[47] Ibrahim, B., Waongo, M., Sidibe, M., Sanfo, S. and Barry, B. (2022) Agroclimatological Characteristics of Rainy Seasons in Southwestern Burkina Faso during the 1970-2013 Period. *Atmospheric and Climate Sciences*, **12**, 330-357. https://doi.org/10.4236/acs.2022.122021

[48] Tian, Y., Peters-Lidard, C.D., Eylander, J.B., Joyce, R.J., Huffman, G.J., Adler, R.F., *et al.* (2009) Component Analysis of Errors in Satellite-Based Precipitation Estimates. *Journal of Geophysical Research*: *Atmospheres*, **114**, D24101. https://doi.org/10.1029/2009jd011949

[49] Frere, M. and Popov, G. (1979) Agrometeorological Crop Monitoring and Forecasting. FAO.

[50] Zhang, X., Alexander, L., Hegerl, G.C., Jones, P., Tank, A.K., Peterson, T.C., *et al.* (2011) Indices for Monitoring Changes in Extremes Based on Daily Temperature and Precipitation Data. *WIREs Climate Change*, **2**, 851-870. https://doi.org/10.1002/wcc.147

[51] Boschetto, R.G., Mohamed, R.M. and Arrigotti, J. (2010) Vulnerability to Desertification in a Sub-Saharan Region: A First Local Assessment in Five Villages of Southern Region of Malawi. *Italian Journal of Agronomy*, **5**, 91-101. https://doi.org/10.4081/ija.2010.s3.91

[52] Steduto, P., Hsiao, T.C., Raes, D. and Fereres, E. (2009) Aquacrop—The FAO Crop Model to Simulate Yield Response to Water: I. Concepts and Underlying Principles. *Agronomy Journal*, **101**, 426-437. https://doi.org/10.2134/agronj2008.0139s

[53] Hartigan, J.A. and Wong, M.A. (1979) Algorithm as 136: A K-Means Clustering Algorithm. *Applied Statistics*, **28**, 100-108. https://doi.org/10.2307/2346830

[54] Sinaga, K.P. and Yang, M. (2020) Unsupervised K-Means Clustering Algorithm. *IEEE Access*, **8**, 80716-80727. https://doi.org/10.1109/access.2020.2988796

[55] Li, Y. and Wu, H. (2012) A Clustering Method Based on K-Means Algorithm. *Physics Procedia*, **25**, 1104-1109. https://doi.org/10.1016/j.phpro.2012.03.206

[56] Bock, H. (2007) Clustering Methods: A History of K-Means Algorithms. In: Bri-to, P., Cucumel, G., Bertrand, P. and de Carvalho, F., Eds., *Studies in Classification, Data Analysis, and Knowledge Organization*, Springer, 161-172. https://doi.org/10.1007/978-3-540-73560-1_15

[57] Humaira, H. and Rasyidah, R. (2020) Determining the Appropiate Cluster Number Using Elbow Method for K-Means Algorithm. *Proceedings of the Proceedings of the* 2*nd Workshop on Multidisciplinary and Applications* (*WMA*) 2018, Padang, 24-25 January 2018. https://doi.org/10.4108/eai.24-1-2018.2292388

[58] Celebi, M.E., Kingravi, H.A. and Vela, P.A. (2013) A Comparative Study of Efficient Initialization Methods for the K-Means Clustering Algorithm. *Expert Systems with Applications*, **40**, 200-210. https://doi.org/10.1016/j.eswa.2012.07.021

[59] Ihaka, R. and Gentleman, R. (1996) R: A Language for Data Analysis and Graphics. *Journal of Computational and Graphical Statistics*, **5**, 299-314. https://doi.org/10.1080/10618600.1996.10474713

[60] Hijmans, R.J. (2020) Terra: Spatial Data Analysis. CRAN: Contributed Packages, The R Foundation. https://doi.org/10.32614/cran.package.terra

[61] Ogihara, M. and Bonnell, J. (2023) Exploring Data Science with R and the Tidyverse: A Concise Introduction. Chapman and Hall/CRC. https://doi.org/10.1201/9781003320845

[62] Waongo, M., Garba, J.N., Diasso, U.J., Sawadogo, W., Sawadogo, W.L. and Daho, T. (2024) A Merging Approach for Improving the Quality of Gridded Precipitation Datasets over Burkina Faso. *Climate*, **12**, Article 226. https://doi.org/10.3390/cli12120226

[63] Nowosad, J. and Stepinski, T.F. (2018) Spatial Association between Regionalizations Using the Information-Theoretical *v*-Measure. *International Journal of Geographical Information Science*, **32**, 2386-2401. https://doi.org/10.1080/13658816.2018.1511794